Multicolor Hybrid Upconversion Nanoparticles and Their Improved Performance as Luminescence Temperature Sensors Due to Energy Transfer

*Rui Chen, Van Duong Ta, Fen Xiao, Qinyuan Zhang, and Handong Sun**

Recently, lanthanide-doped upconversion nanoparticles (UCNPs) have attracted growing research interest owing to their potential application in upconversion lasers, solar cells, biological labeling, and in vivo imaging.[1–9] Compared to conventional fluorescence imaging based on single-photon excitation, upconversion imaging possesses advantages such as minimum photodamage to living cells, weak autofluorescence from the background environment, high detection sensitivity, and large penetration depth into tissues.[10] Until now, among various lanthanide-doped upconversion materials, hexagonal-phase $NaYF_4$:Yb,Er has been recognized as the most efficient one in which the Yb^{3+} ions absorb multiple near-infrared (NIR) photons while the Er^{3+} ions emit visible light.[11] Research has been carried out to modify the surface properties and enhance the emission.[12–16] However, the further practical application of UCNPs is still limited due to their color tunability.[17]

Förster resonance energy transfer (FRET) is a nonradiative process characterized by energy transfer between excited donors and acceptors through long-range dipole–dipole interaction. It is widely used as a spectroscopic ruler, in biological detection, and in photodynamic therapy.[18,19] Based on this mechanism, efforts have been devoted to encapsulate UCNPs with organic dye molecules or colloidal quantum dots (QDs), and multicolor emission and ratiometric multiplexed encoding have been demonstrated.[10,20,21] As is well known, organic dye molecules are widely used as donor or acceptor in FRET detection or imaging. Moreover, it is found that they have advantages such as small molecular volume, good biocompatibility, bioselectivity, and high fluorescence efficiency.[22,23] Therefore, in the study reported herein, we present a simple but effective approach to achieving multicolor emission from $NaYF_4$:(20% Yb^{3+} and 2% Er^{3+}) UCNPs to rhodamine 6G (R6G) dye molecules based on energy transfer. Dye concentration-dependent and time-resolved photoluminescence (TRPL) measurements were carried out to determine the energy-transfer process inside the hybrid complexes. Moreover, hemispherical microstructures made from the hybrid nanoparticles were created through a hydrophobic effect. A new temperature sensor based on luminescence intensity was proposed and demonstrated, by taking advantage of the high temperature sensitivity of the UCNP+R6G complexes.

As shown in **Figure 1**a, the UCNPs have uniform size distribution with an edge length of around 150 nm. From

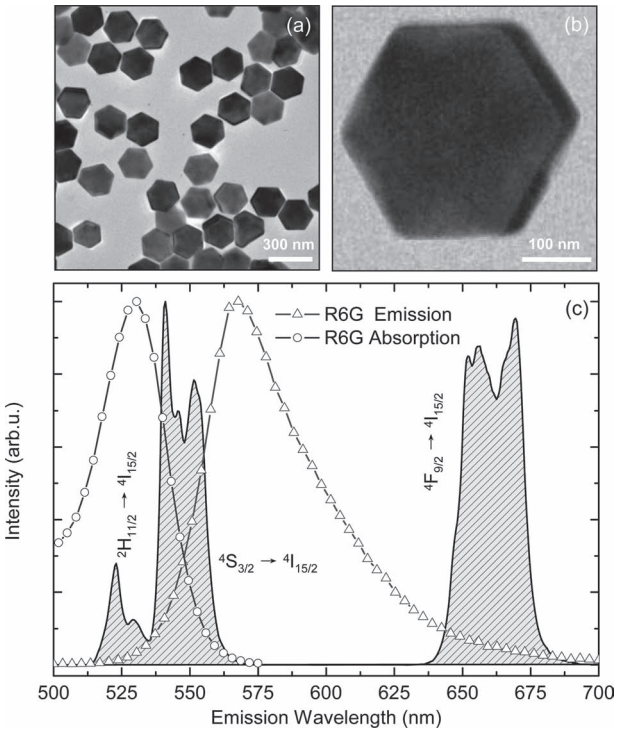

Figure 1. a) FESEM image of $NaYF_4$:(20% Yb^{3+} and 2% Er^{3+}). b) Close-up FESEM image showing the hexagonal shape of the UCNP. c) Upconversion emission from UCNPs (filled spectrum) under NIR laser excitation. The absorption and emission from R6G are presented for comparison.

Dr. R. Chen, V. D. Ta, Dr. F. Xiao, Prof. H. D. Sun
Division of Physics and Applied Physics
School of Physical and Mathematical Sciences
Nanyang Technological University
Singapore 637371, Singapore
E-mail: hdsun@ntu.edu.sg
Prof. H. D. Sun
Centre for Disruptive Photonic Technologies (CDPT)
Nanyang Technological University, Singapore
Dr. F. Xiao, Prof. Q. Y. Zhang
State Key Laboratory of Luminescent
Materials and Devices
and Institute of Optical Communication Materials
South China University of Technology
Guangzhou 510641, PR China

DOI: 10.1002/smll.201202287

small NANO MICRO

the close-up field-emission scanning electron microscopy (FESEM) image in Figure 1b, it can be seen clearly that the disk has a perfect hexagonal shape, which implies highly directional growth and the high quality of the sample. The thickness of the hexagonal disk was estimated to be around 27 nm. Under continuous-wave (CW) NIR laser excitation, the sample exhibits strong upconverted photoluminescence (PL), which can be observed even with the naked eye, and a typical PL spectrum is presented in Figure 1c. The characteristic green and red emissions can be identified as from electronic transitions from the energy levels $^2H_{11/2}$, $^4S_{3/2}$, and $^4F_{9/2}$ to $^4I_{15/2}$ of Er^{3+} ions.[1,24] The normalized absorption and emission spectra of the R6G dye molecules are given for comparison. It could be expected that energy transfer between UCNPs and R6G would take place because the green emission of the donor (UCNP) overlaps with the absorption band of the acceptor (R6G).[10] It should be mentioned that no emission from pure R6G can be detected under excitation at 980 nm because there is almost no absorption at this wavelength. Meanwhile, the red emission from UCNPs does not overlap with the R6G dye emission, which would facilitate the assessment of the energy-transfer process.

R6G dye molecules were dissolved in dimethyl sulfoxide (DMSO) and then mixed with UCNPs to form the complexes. **Figure 2**a plots the PL emission from the complexes with different R6G concentration. All spectra were normalized at red emission (640–680 nm) for the convenience of comparison. It can be seen that by increasing the dye concentration, the green erbium emission at 525–560 nm decreases, while the emission band around 575 nm from the dye emerges. Simultaneously, the dye emission peak demonstrates a gradual redshift, which can be explained by the reabsorption effect.[25] To see the influence of dye concentration on the PL properties more clearly, the ratios of integrated PL intensity of the green emission from UCNPs and R6G compared to the red emission from UCNPs is plotted in Figure 2b. Once again, a 75% decrease of the ratio green/red and 30% increase of the ratio R6G/red can be determined. The decrease of the green emission from UCNPs could originate from various factors, such as surface-to-volume ratio, excitation power, size and shape of the UCNPs, as well as the concentration of Yb^{3+} and Er^{3+} ions.[26] As the PL measurements were performed under identical conditions, the above-mentioned possibilities can be ruled out and the emission decrease is ascribed to the increase of dye concentration. The CIE chromaticity diagram is shown in Figure 2c, in which the symbols denote the color position of the UCNP complex with increased dye concentration. It can be seen that the color changes from yellow-green to peach-buff as the concentration of the dye increases, which clearly demonstrates the color tunability of the hybrid complexes.

As mentioned before, under NIR excitation there is no emission from R6G. Therefore, the observed color change of the complexes implies the existence of energy transfer. Actually, for donor and acceptor with spectral overlap, the energy transfer can be realized by either nonradiative energy transfer (FRET) or radiative energy transfer (radiative recombination in the donor first and then reabsorption by the acceptor).[22] To distinguish the two processes, TRPL measurement monitoring the donor emission (green emission from UCNPs) was carried out and the results are depicted in **Figure 3**a. The decay curves can be well fitted by exponential fitting with reconvolution:[27]

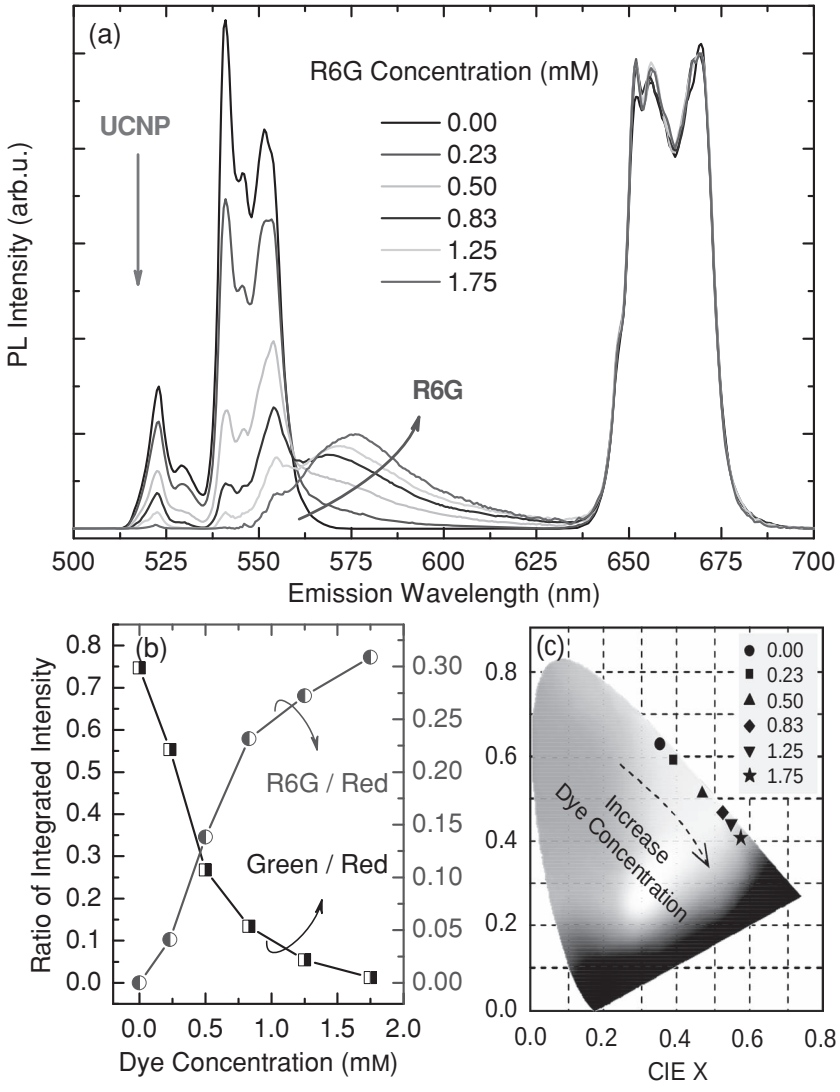

Figure 2. a) Upconversion emission from UCNPs with different dye concentration. b) Ratios of the integrated PL intensity between the green emission from UCNPs and R6G compared to the red emission from UCNPs. c) CIE chromaticity diagram of the emissions, in which the symbols denote the color position of UCNPs and the corresponding dye concentrations (in mM) are given.

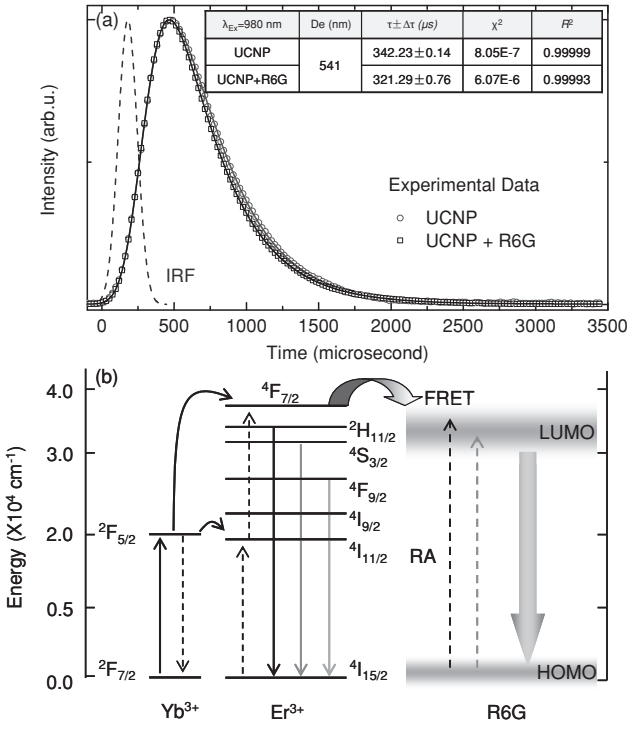

Figure 3. a) TRPL of UCNPs with and without R6G. IRF is the instrument response function. The fitted data are presented in the inset table. The decay curves are detected at 541 nm. τ is the lifetime, and χ^2 and R^2 are the chi-squared and *R*-squared values of the fitting, respectively. b) Schematic diagram illustrating the possible mechanism of the emission and energy-transfer process.

$$I(t) = \int_{-\infty}^{t} \mathrm{IRF}(t') A e^{-(t-t')/\tau} \mathrm{d}t' \quad (1)$$

where A is the amplitude of the component at time zero, τ is the corresponding lifetime, and IRF is the instrument response function. The table inserted in Figure 3a summarizes the fitting information and the decays obtained. The data clearly show a decreased lifetime in the presence of R6G in UCNPs, which is 342 and 321 μs for UCNPs without and with R6G dye molecules, respectively. Such a reduced lifetime provides direct evidence that FRET does exist in the hybrid complexes because FRET acts as an extra energy-decay channel. From the decay curves, the efficiency of energy transfer (η_{ET}) can be calculated from the following equation:[28,29]

$$\eta_{ET} = 1 - \tau/\tau_0 \quad (2)$$

where τ and τ_0 are the lifetime of UCNPs with and without R6G doping, respectively. According to the data extracted, the energy-transfer efficiency of the complexes is determined to be only 6.12%. It is reported that the Förster radius is around 1.5 nm for UCNPs with colloidal CdSe QDs.[21,30] In our material system, the acceptor (R6G dye molecule) is present in DMSO solution and thus is highly diluted. From a statistical point of view, only a minor fraction of the dissolved dye is within the rather small Förster distance, while most dye is far away. As a result, FRET occurs mostly between Er^{3+} ions near the surface of the nanoparticles and the nearby dye molecules in the solution. The emission from ions inside UCNPs contributes to the radiative energy transfer due to photon reabsorption.

On the basis of the results obtained above, a schematic diagram is depicted in Figure 3c to illustrate the possible mechanism of the emission and energy-transfer process. Under NIR excitation, the $^4F_{7/2}$ level in Er^{3+} is populated via an energy-transfer upconversion process. This energy can then relax nonradiatively to the $^2H_{11/2}$, $^4S_{3/2}$, and $^4F_{9/2}$ levels, then green $^2H_{11/2} \rightarrow {}^4I_{15/2}$ (525 nm), $^4S_{3/2} \rightarrow {}^4I_{15/2}$ (545 nm), and red emission of $^4F_{9/2} \rightarrow {}^4I_{15/2}$ (660 nm) occur. Some of the emitted photons from the transitions of $^2H_{11/2} \rightarrow {}^4I_{15/2}$ (525 nm) and $^4S_{3/2} \rightarrow {}^4I_{15/2}$ may be reabsorbed (RA) by the R6G, and excite the electrons in R6G from the highest occupied molecular orbital (HOMO) to the lowest unoccupied molecular orbital (LUMO). Simultaneously, due to the spectral overlap, part of the energy will resonantly transfer from Er^{3+} ions to R6G. Finally, those carriers in the LUMO recombine radiatively and give rise to the intense dye emission.

For the photonic device, various applications such as NIR photodetector and optical sensor based on UCNPs have been demonstrated.[31–34] Among them, optical temperature sensors are very important for biomedical use due to their fast response, reversibility, and the possibility to realize nanoscale spatial resolution.[32,35] Until now, most optical temperature sensors have been based on the fluorescence intensity ratio (FIR) technique.[36] For UCNPs, temperature will influence the carrier population in different energy levels of the ion, while the emission positions remain unchanged. Therefore, a sample's temperature can be determined by comparing different peak intensities. However, one needs to monitor different emission intensities and carry out necessary mathematical calculation, which is not straightforward and will introduce large errors. Herein, we propose and demonstrate a simpler approach to detecting temperature precisely down to the microscale, by using hemispherical microstructures containing the UCNPs and R6G.

To create the hemispherical microstructure, UCNPs and R6G were dissolved in epoxy resin (Araldite 506 from Sigma–Aldrich) with a suitable amount of chloroform ($CHCl_3$). As schematically illustrated in **Figure 4**a, the solution containing UCNPs and R6G forms multiple droplets on a fiber tip coated with hydrophobic material. The droplets can be transferred onto the substrate by approaching the fiber tip to the substrate. Due to the hydrophobic property of the substrate, self-assembled hemispherical microstructures will be formed spontaneously by surface tension.[37,38] A smaller size of hemispherical structure can be obtained by subsequent deposition using the same fiber tip. As shown in the optical images in Figure 4b–e, hemispherical microstructures with diameters from 150 to 25 μm can be obtained. The experimental configuration for the subsequent temperature sensing is shown in Figure 4f. Briefly, the upconverted emission from the microstructure was collected by a microscope and delivered to a spectrometer via an optical fiber. A heater with controllable position and temperature was used to vary the temperature.

small NANO MICRO

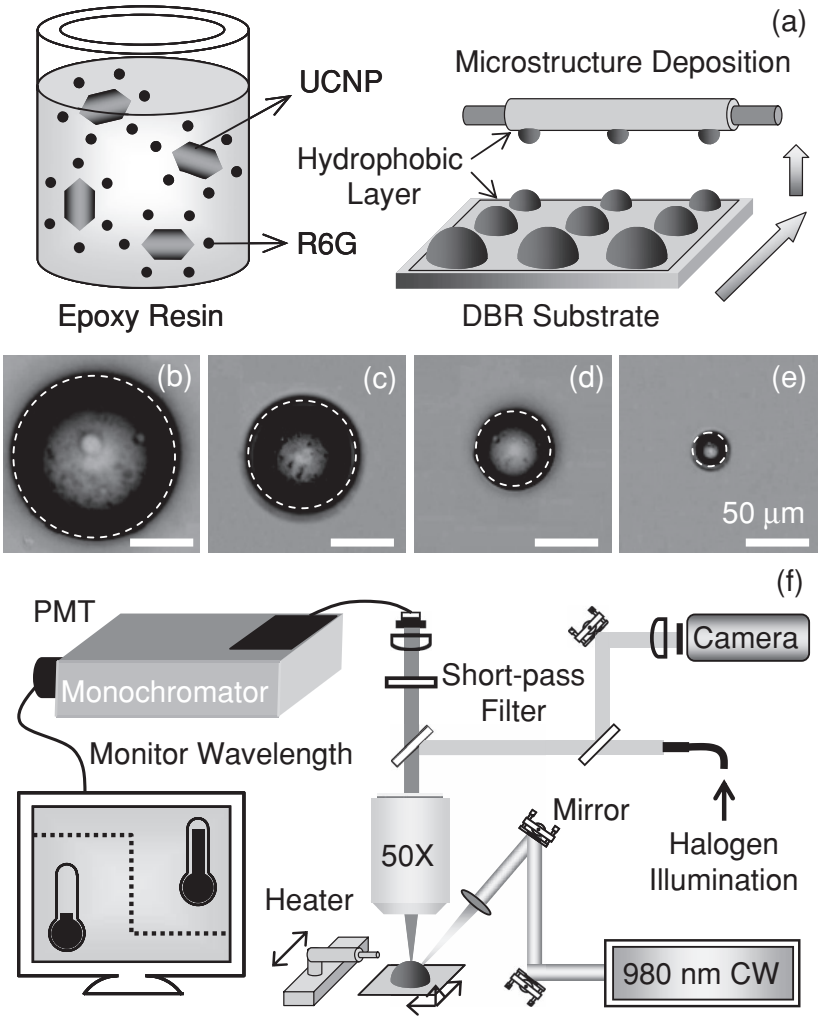

Figure 4. a) Schematic diagram showing the fabrication of hemispherical microstructures based on the hydrophobic effect. b–e) Top-down view optical images of microstructures with different sizes under halogen illumination; scale bars: 50 μm. f) Schematic of experimental setup for the temperature sensing of individual microstructures. DBR=distributed Bragg reflector, PMT=photomultiplier tube.

It is found that the hemispherical microstructure with dye-doped UCNPs exhibits PL emission similar to that in solution (data not shown). The spectrometer was set to monitor the emission intensity from R6G at 575 nm while the environmental temperature was changing. **Figure 5**a shows the change of PL intensity under different temperatures. It can be seen that when the environmental temperature increases to 5 °C above room temperature, the PL emission from R6G decreases by 4.5%. The PL intensity keeps decreasing with the increase of temperature, which can be as high as nearly 50% at 30 °C above room temperature. From the data plotted, it is noted that the temperature response of the sample is quick, stable, and reversible. The inset of Figure 5a presents the percentage of PL intensity decrease as a function of temperature. From the linear fitting, the average temperature sensitivity is estimated to be 1% per °C over the whole physiological temperature range (25–45 °C) and 2.7% per °C in the higher-temperature region (47–57 °C).[39]

PL intensities from the dye (575 nm) and red emission from UCNPs (660 nm) were recorded at 25 °C above room temperature. From the data plotted in Figure 5b, it can be seen that the dye emission decreases by 30% whereas the red emission from UCNPs only decreases by 11%. Compared with rare-earth ions, dye molecules possess a stronger temperature-dependent absorption and emission. As mentioned previously, dye in the hybrid complexes harvests its energy only from UCNPs through energy transfer. Therefore, the emission from UCNPs, the absorption/emission from the dye, as well as the energy-transfer efficiency influenced by temperature should be responsible for the higher temperature sensitivity observed in the hybrid complexes. To verify this hypothesis, microstructures formed by pure UCNPs were created. Figure 5c demonstrates the green (545 nm) and red emission (660 nm) from UCNPs under the same conditions as a function of time. The temperature response of the red emission from UCNPs remains unchanged, because the emission is not influenced by the dye doping. However, the PL intensity of the green emission from UCNPs decreases by only 15%. Once again, the superior property of the complexes strongly supports the existence of energy transfer during the optical process. Based on the observations obtained above, we can conclude that energy transfer is the main reason for the improved temperature sensitivity in the UCNP and R6G complexes. Following this idea, temperature information can be obtained during the upconversion imaging process, which is helpful for biomedical research.

In conclusion, we have investigated the optical properties of UCNP and R6G hybrid complexes. By changing the dye concentration, multicolor emission from the sample can be achieved. From the TRPL, we found that both FRET and radiative energy transfer exist during the optical process. Finally, self-assembled hemispherical microstructures containing the complexes were fabricated through a hydrophobic effect, and their temperature response was examined. It was found that the complexes demonstrate better temperature sensitivity than the pure UCNPs, which is due to the energy transfer between UCNPs and R6G. Based on this idea, temperature sensing down to the microscale can be realized. Our investigation not only reveals the unique optical properties and mechanism of the UCNP+R6G complexes, but also demonstrates their potential application as a temperature sensor. Research along these lines may help to advance functional material applications in biomedical research.

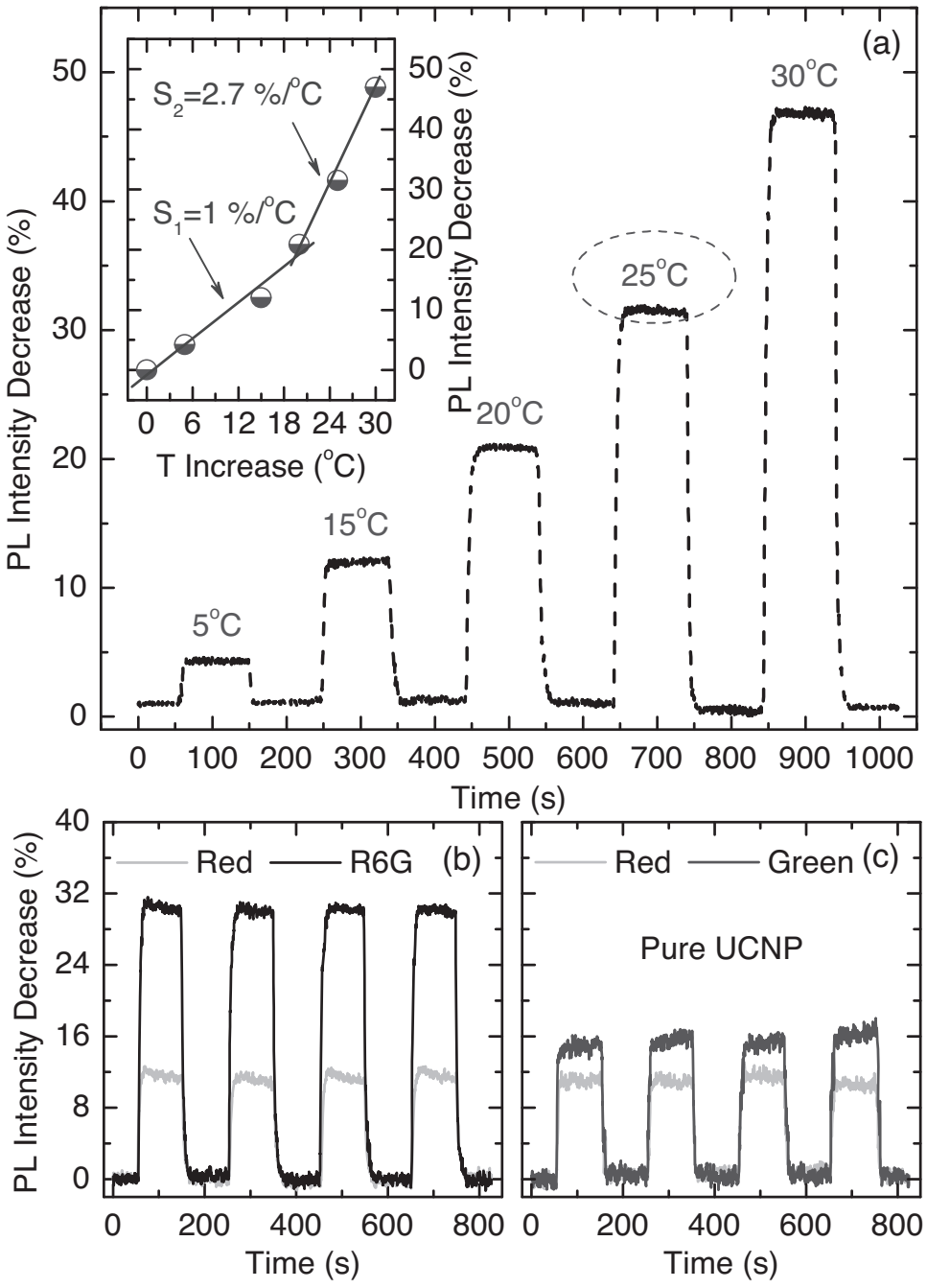

Figure 5. a) Decrease of emission from R6G as a function of time and environmental temperature. Inset: the emission intensity change under different temperatures. b) PL intensity change from the dye and red emission from UCNPs recorded at 25 °C above room temperature. c) PL intensity change from green and red emission of pure UCNPs under identical conditions.

Experimental Section

Materials Synthesis: The UCNPs used herein were prepared by a modified hydrothermal process. First, $RECl_3$ (0.4 mmol; RE = Y^{3+}, Yb^{3+}, Er^{3+}) was added to a flask containing a mixture of 1-octadecene and oleic acid. The solution was heated to 160 °C for 30 min under argon protection and then cooled to room temperature. Subsequently, a methanol solution (5 mL) of NH_4F (1.6 mmol) and NaOH (1 mmol) was added to the flask and the resulting mixture was stirred for 30 min. After removal of the methanol by evaporation, the solution was heated to 310 °C under an argon environment for 1 h and cooled to room temperature. The resulting $NaYF_4$:(20% Yb^{3+} and 2% Er^{3+}) nanoparticles were precipitated by the addition of ethanol, collected by centrifugation, washed with water and ethanol several times, and finally dispersed in DMSO.

Optical Measurements: Samples were prepared by placing a drop containing the sample on the surface of a copper grid. PL measurements were performed at room temperature and a 2.5 W CW diode laser emitting at 980 nm was used as the excitation source. During the measurement, emission of the sample was

small NANO MICRO

collected from the edge to reduce the influence of the laser beam. The signal was dispersed by a 750 mm monochromator combined with suitable filters, and detected by a photomultiplier tube (Hamamatsu R928) using a standard lock-in amplifier technique. For the TRPL, the chopper wheel was replaced by a homemade one and the repetition rate of the mechanical chopper was maintained at 500 Hz to generate pulses with a pulse width of 0.15 ms. The detector output was stored on a digital phosphor oscilloscope (Tektronix DPO 7254) and averaged over 500 periods to improve the signal-to-noise ratio.

Acknowledgements

Support from the Singapore Ministry of Education through the Academic Research Fund (Tier 1) under Project No. RG63/10 and from the Singapore National Research Foundation through the Competitive Research Programme (CRP) under Project Nos. NRF-CRP5-2009-04 and NRF-CRP6-2010-02 is gratefully acknowledged.

[1] F. Auzel, *Chem. Rev.* **2003**, *104*, 139.
[2] P. Reiss, M. Protière, L. Li, *Small* **2009**, *5*, 154.
[3] F. Wang, Y. Han, C. S. Lim, Y. Lu, J. Wang, J. Xu, H. Chen, C. Zhang, M. Hong, X. Liu, *Nature* **2010**, *463*, 1061.
[4] M. Haase, H. Schäfer, *Angew. Chem. Int. Ed.* **2011**, *50*, 5808.
[5] S. Heer, K. Kömpe, H. U. Güdel, M. Haase, *Adv. Mater.* **2004**, *16*, 2102.
[6] D. Tu, L. Liu, Q. Ju, Y. Liu, H. Zhu, R. Li, X. Chen, *Angew. Chem. Int. Ed.* **2011**, *50*, 6306.
[7] T. He, W. Wei, L. Ma, R. Chen, S. Wu, H. Zhang, Y. Yang, J. Ma, L. Huang, G. G. Gurzadyan, H. Sun, *Small* **2012**, *8*, 2163.
[8] S. Jiang, Y. Zhang, *Langmuir* **2010**, *26*, 6689.
[9] D. E. Achatz, R. Ali, O. S. Wolfbeis, *Top. Curr. Chem.* **2011**, *300*, 29.
[10] Z. Li, Y. Zhang, S. Jiang, *Adv. Mater.* **2008**, *20*, 4765.
[11] K. W. Krämer, D. Biner, G. Frei, H. U. Güdel, M. P. Hehlen, S. R. Lüthi, *Chem. Mater.* **2004**, *16*, 1244.
[12] S. Schietinger, T. Aichele, H.-Q. Wang, T. Nann, O. Benson, *Nano Lett.* **2009**, *10*, 134.
[13] W. Deng, L. Sudheendra, J. B. Zhao, J. X. Fu, D. Y. Jin, I. M. Kennedy, E. M. Goldys, *Nanotechnology* **2011**, *22*, 325604.
[14] L. Wang, R. Yan, Z. Huo, L. Wang, J. Zeng, J. Bao, X. Wang, Q. Peng, Y. Li, *Angew. Chem. Int. Ed.* **2005**, *44*, 6054.
[15] Z. Li, L. Wang, Z. Wang, X. Liu, Y. Xiong, *J. Phys. Chem. C* **2011**, *115*, 3291.
[16] T. Rantanen, H. Päkkilä, L. Jämsen, K. Kuningas, T. Ukonaho, T. Lövgren, T. Soukka, *Anal. Chem.* **2007**, *79*, 6312.
[17] L. Cheng, K. Yang, M. Shao, S.-T. Lee, Z. Liu, *J. Phys. Chem. C* **2011**, *115*, 2686.
[18] R. Bakalova, H. Ohba, Z. Zhelev, M. Ishikawa, Y. Baba, *Nat. Biotechnol.* **2004**, *22*, 1360.
[19] L. Stryer, R. P. Haugland, *Proc. Natl. Acad. Sci. USA* **1967**, *58*, 719.
[20] H. H. Gorris, R. Ali, S. M. Saleh, O. S. Wolfbeis, *Adv. Mater.* **2011**, *23*, 1652.
[21] A. Bednarkiewicz, M. Nyk, M. Samoc, W. Strek, *J. Phys. Chem. C* **2010**, *114*, 17535.
[22] R. Chen, Y. Q. Shen, F. Xiao, B. Liu, G. G. Gurzadyan, Z. L. Dong, X. W. Sun, H. D. Sun, *J. Phys. Chem. C* **2010**, *114*, 18081.
[23] F. Xiao, R. Chen, Y. Q. Shen, Z. L. Dong, H. H. Wang, Q. Y. Zhang, H. D. Sun, *J. Phys. Chem. C* **2012**, *116*, 13458.
[24] J.-C. Boyer, L. A. Cuccia, J. A. Capobianco, *Nano Lett.* **2007**, *7*, 847.
[25] T. C. He, R. Chen, W. W. Lin, F. Huang, H. D. Sun, *Appl. Phys. Lett.* **2011**, *99*, 081902.
[26] J. Shan, M. Uddi, R. Wei, N. Yao, Y. Ju, *J. Phys. Chem. C* **2010**, *114*, 2452.
[27] R. Chen, D. Li, B. Liu, Z. Peng, G. G. Gurzadyan, Q. Xiong, H. Sun, *Nano Lett.* **2010**, *10*, 4956.
[28] S. A. Crooker, J. A. Hollingsworth, S. Tretiak, V. I. Klimov, *Phys. Rev. Lett.* **2002**, *89*, 186802.
[29] F. Xiao, R. Chen, Y. Q. Shen, B. Liu, G. G. Gurzadyan, Z. L. Dong, Q. Y. Zhang, H. D. Sun, *J. Alloys Compd.* **2011**, *509*, 7794.
[30] L. J. Charbonnière, N. Hildebrandt, R. F. Ziessel, H.-G. Löhmannsröben, *J. Am. Chem. Soc.* **2006**, *128*, 12800.
[31] C. Yan, A. Dadvand, F. Rosei, D. F. Perepichka, *J. Am. Chem. Soc.* **2010**, *132*, 8868.
[32] B. Dong, B. Cao, Y. He, Z. Liu, Z. Li, Z. Feng, *Adv. Mater.* **2012**, *24*, 1987.
[33] L. H. Fischer, G. S. Harms, O. S. Wolfbeis, *Angew. Chem. Int. Ed.* **2011**, *50*, 4546.
[34] D. E. Achatz, R. J. Meier, L. H. Fischer, O. S. Wolfbeis, *Angew. Chem. Int. Ed.* **2011**, *50*, 260.
[35] P. Löw, B. Kim, N. Takama, C. Bergaud, *Small* **2008**, *4*, 908.
[36] P. V. dos Santos, M. T. de Araujo, A. S. Gouveia-Neto, J. A. M. Neto, A. S. B. Sombra, *Appl. Phys. Lett.* **1998**, *73*, 578.
[37] V. D. Ta, R. Chen, H. D. Sun, *Adv. Mater.* **2012**, *24*, OP60.
[38] R. Chen, V. D. Ta, H. D. Sun, *Sci. Rep.* **2012**, *2*, 244.
[39] L.-N. Sun, J. Yu, H. Peng, J. Z. Zhang, L.-Y. Shi, O. S. Wolfbeis, *J. Phys. Chem. C* **2010**, *114*, 12642.

Received: September 17, 2012
Revised: November 2, 2012
Published online: January 4, 2013

